ACS Medicinal Chemistry Letters

Letter

pubs.acs.org/acsmedchemlett

Structural Insights for the Optimization of Dihydropyrimidin-2(1*H*)-one Based mPGES-1 Inhibitors

Stefania Terracciano,[†] Gianluigi Lauro,[†] Maria Strocchia,[†] Katrin Fischer,[‡] Oliver Werz,[‡] Raffaele Riccio,[†] Ines Bruno,*[,†] and Giuseppe Bifulco*[,†]

[†]Department of Pharmacy, University of Salerno, via Giovanni Paolo II, 132, 84084 Fisciano (SA), Italy

[‡]Department of Pharmaceutical/Medicinal Chemistry, Institute of Pharmacy, Friedrich Schiller University, Jena, Philosophenweg 14, D-07743 Jena, Germany

Supporting Information

ABSTRACT: The recently crystallized structure of microsomal prostaglandin E_2 synthase 1 (mPGES-1) in complex with the inhibitor LVJ (PDB code: 4BPM) offered new structural information for the optimization of the previously identified lead compound **1** (IC_{50} = 4.16 ± 0.47 μM), which contains the privileged dihydropyrimidin-2-one chemical core. Systematic optimization of **1**, through accurate structure-based design, provided compound **4** with a 10-fold improved mPGES-1 inhibitory activity (IC_{50} = 0.41 ± 0.02 μM). Here we highlight the optimal scaffold decoration pattern of **4** and propose a three-dimensional model for the interaction with this complex trimeric membrane protein. The reported computational insights, together with the accessible one-pot synthetic procedure, stimulate for the generation of further potent dihydropyrimidine-based mPGES-1 inhibitors.

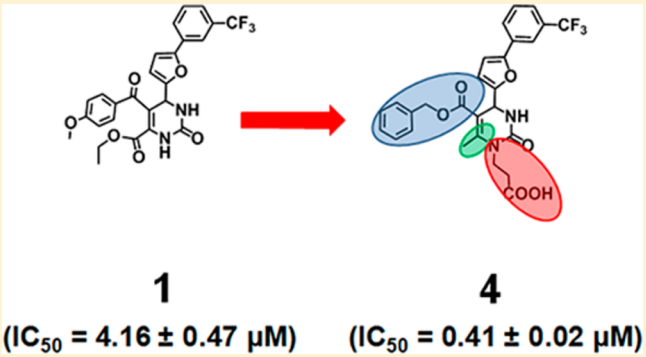

KEYWORDS: *Molecular docking, inflammation, mPGES-1 inhibitors, Biginelli reaction*

Prostaglandin E_2 synthases (mPGES-1, mPGES-2, and cPGES) are the terminal enzymes involved in the biosynthesis of the crucial inflammatory lipid mediator PGE_2.[1] Unlike the constitutive forms (mPGES-2 and cPGES), the inducible membrane-bound isoform mPGES-1 has emerged as a strategic drug target in PGE_2-related acute and chronic disorders,[2] such as inflammation,[3] pain,[4] fever,[5] rheumatoid arthritis,[6] osteoarthritis,[7] and cancer.[8,9]

The main limitations connected to the use of classical anti-inflammatory drugs (NSAIDs and coxibs), which reduce PGE_2 levels by blocking COX enzymes, are cardiovascular, gastrointestinal, and renal side effects; hence, there is a strong need to develop safer alternatives especially for long-term therapies.[10,11] In this field, mPGES-1 inhibitors could represent a valuable pharmacological approach without affecting the formation of PGH_2 enzymatically produced by the COXs. Up to now, a number of compounds with different chemotypes have been identified, but none have entered clinical trials.[12,13] Structural information on the key functional groups, including a defined pharmacophore, has been the major issue for the development of potent mPGES-1 inhibitors through rational design approaches. In addition, the first detailed information about the three-dimensional structure of this glutathione-dependent protein in the active form were only recently provided by means of X-ray experiments by Sjögren et al. in 2013.[14] The determined structure revealed that the mPGES-1 homotrimer has three active site cavities within the membrane-spanning region at each monomer interface. The asymmetric monomer is formed by a four-helix bundle, and each active site is between the N-terminal parts of helix II and IV of a monomer, the C-terminal part of helix I, and the cytoplasmic domain of the adjacent monomer, toward the cytoplasmic part of the protein (Figure 1). The cofactor (GSH) adopts a U-shape due to the strong interactions between its two terminal carboxylic functions and a positively charged region in the deeper part of the binding site.

As previously reported, we have recently uncovered a rational design approach for the discovery of new mPGES-1 inhibitors featuring the dihydropyrimidin-2(1)*H*-one (DHPM) core, by using the above-described crystal structure.[15] In that work, we performed molecular docking studies and identified the promising candidate **1** (IC_{50} = 4.16 ± 0.47 μM, Scheme 1) as mPGES-1 inhibitor featuring the new DHPM chemical core.

In 2014, a new high-resolution X-ray structure of human mPGES-1 in lipidic mesophase has been reported in a structural biology study in complex with the highly potent inhibitor LVJ (2-[[2,6-bis(chloranyl)-3-[(2,2dimethylpropanoylamino)-methyl]phenyl]amino]-1-methyl-6-(2-methyl-2-oxidanyl-propoxy)-*N*-[2,2,2-tris(fluoranyl)ethyl]benzimidazole-5-carboxa-

Received: October 24, 2014
Accepted: January 7, 2015
Published: January 7, 2015

DOI: 10.1021/ml500433j
ACS Med. Chem. Lett. 2015, 6, 187−191

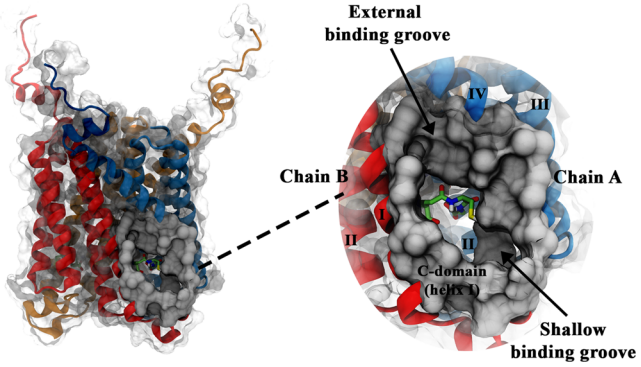

Figure 1. Microsomal prostaglandin synthase-1 (mPGES-1) structure (PDB code: 4BPM) (secondary structure: chain A blue; chain B red; chain C orange). Glutathione as cofactor is depicted in licorice mode (C, green; O, red; N, blue; H, light gray), molecular surface focused to the binding site colored in gray.

Scheme 1. Structures of Compounds 1−4 and Synthetic Strategy

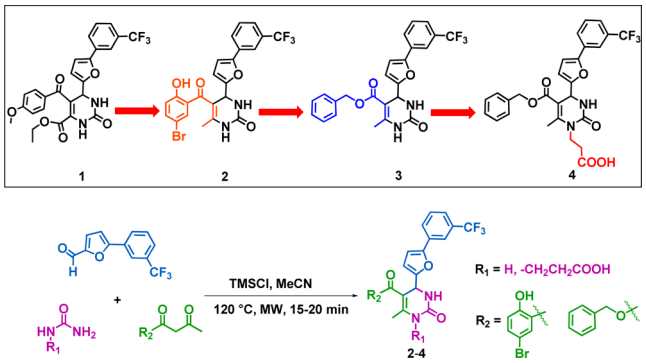

mide) (PDB code: 4BPM).[16] Since it was the first reported cocrystal ligand−protein structure, we undertook a careful analysis of the binding mode of LVJ in order to get useful information and to clarify the molecular basis for interaction of a mPGES-1 inhibitor with the receptor counterpart. First, LVJ acts as a substrate competitive inhibitor but is unable to displace the cofactor GSH. We analyzed the three-dimensional model (Figure 2) and noticed an extended set of polar and hydrophobic interactions of LVJ with the key residues responsible for the catalytic activity of the investigated protein (A:ARG126, A:SER127, and A:THR131). Importantly, LVJ adopts a peculiar slumped shape in the binding site, and this is mainly due to a strong edge-to-face $\pi-\pi$ interaction between its dichlorophenyl moiety and the phenyl group in the side chain of B:PHE44, and similarly with B:HIS53 (Figure 2). Moreover, the substituted benzimidazole moiety interacts with the external part of the binding site toward chain A, and the smaller (2,2-dimethylpropanoylamino)-methyl linear substituent partially occupies the binding groove in the upper portion of the active site (Figure 2).

In light of the new elucidated structural insights, we re-evaluated the binding mode of our lead compound **1** (Scheme 1) with this new X-ray mPGES-1 structure by means of molecular docking experiments. In particular, in our previous model, we underlined the importance of the 4-methoxybenzoyl group at C5 duly oriented on the central dihydropyrimidin-2(1*H*)-one core, that when absent, dropped the inhibitory activity due to the failure of establishing key interactions with the receptor counterpart. Moreover, we identified a fundamental face-to-face $\pi-\pi$ interaction between this aromatic moiety and the A:TYR130, the latter being normally involved in a stable contact with the cofactor GSH promoting the catalytic process.[14]

In the new model here proposed, we evaluated the binding mode of **1** in the presence of GSH (as LVJ), and we found that the main feature of this new model is the different orientation of the 4-methoxybenzoyl group at C5 (Figure S1, Supporting Information). In particular, while the 5-(3-(trifluoromethyl)-phenyl)furan-2-yl group at C4 occupies the binding groove in a similar manner, in our new model the aromatic ring at C5 is oriented toward the shallow binding groove on the cytoplasmic part of the protein, close to the B:PHE44. Nevertheless, although the compound is able to occupy the binding site by establishing a large pattern of contacts, the strong edge-to-face

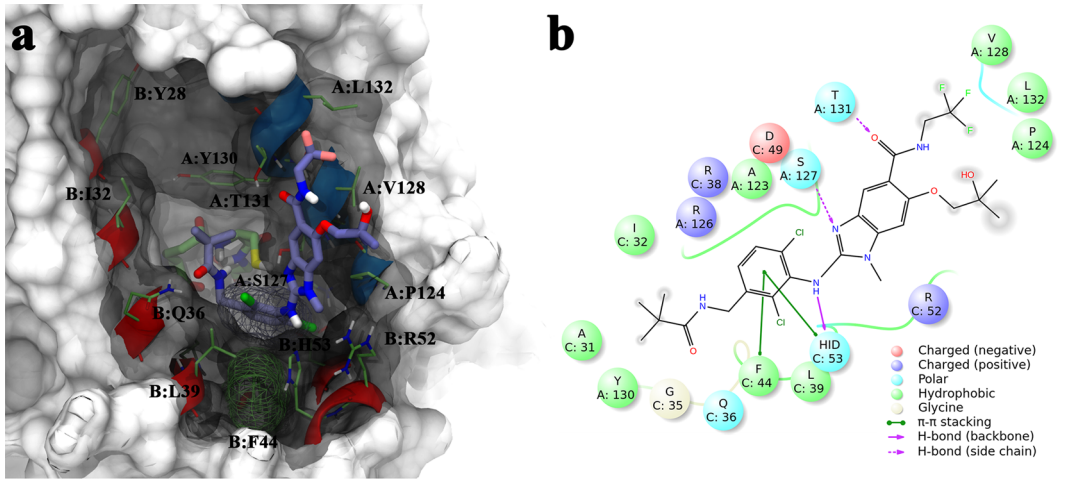

Figure 2. (a) Three-dimensional model of LVJ (colored by atom types: C, iceblue; N, blue; O, red; H, light gray; Cl, green; F, pink) in the mPGES-1 binding site (molecular surface represented in white); residues in the active site represented in licorice (colored by atom types: C, green; N, blue; O, red; S, yellow; H, light gray) and related molecular surfaces depicted in transparent silver; molecular surfaces of the interacting chemical groups of LVJ and B:PHE44 (edge-to-face $\pi-\pi$ interaction) are highlighted in wireframes. (b) Two-dimensional panel representing interactions between LVJ and residues in mPGES-1 binding site.

DOI: 10.1021/ml500433j
ACS Med. Chem. Lett. 2015, 6, 187−191

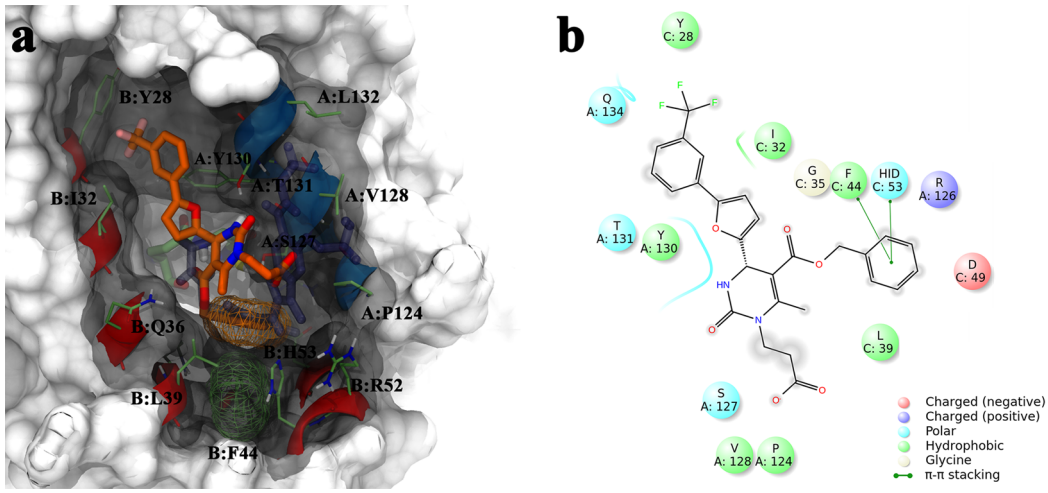

Figure 3. (a) Three-dimensional model of **4** (colored by atom types: C, orange; N, blue; O, red; H, light gray; F, pink) in docking with mPGES-1 (molecular surface represented in white); residues in the active site represented in licorice (colored by atom types: C, green; N, blue; O, red; S, yellow; H, light gray) and related molecular surfaces depicted in transparent silver; molecular surfaces of the interacting chemical groups of **4** and B:PHE44 (edge-to-face $\pi-\pi$ interaction) are highlighted in wireframes; the superimposed structure of LVJ is depicted in transparent iceblue licorice. (b) Two-dimensional panel representing interactions between **4** and residues in mPGES-1 binding site.

$\pi-\pi$ interaction with B:PHE44, observed for LVJ, is not detectable in this case (Figure S1, Supporting Information).

In an effort to improve the activity of our lead compound, we focused in designing and synthesizing three structural related analogues of **1** (compounds **2**–**4**), thus considering it as reference compound and making precise and accurate slight modifications. In these new molecules, we preserved the 5-(3-(trifluoromethyl)phenyl)-furan-2-yl group at C4 because of its good shape complementarity with the enzyme, we modified the aromatic substituent at C5 to reach B:PHE44, and finally we simplified the C6 position of the DHPM core, which was not essential for the protein inhibition.

By exploiting our optimized protocol for the synthesis of DHPMs, we obtained compounds **2**–**4** in very easy and fast experimental conditions. As alternative to conventional linear-type strategies, we relied again on the Biginelli three-component dihydropyrimidine condensation, a useful approach in diversity-oriented synthesis in organic and medicinal chemistry,[17,18] thanks to its speed, efficiency, and high-yields.[19] Although this chemical procedure is suitable in producing large collections of diverse molecules, the main aim of this study was to employ the new mPGES-1 structural information for the optimization of lead compound **1**, without altering its pharmacophoric portions. For these reasons, we used three commercially available Biginelli building blocks in a microwave-assisted procedure and accomplished the synthesis of compounds **2**–**4**, as outlined in Scheme 1. Once again, a high-speed microwave-assisted trimethylsilyl chloride (TMSCl)-mediated Biginelli condensation provided a rapid access to the desired dihydropyrimidine derivatives in good yields and short reaction times. Synthesized compounds were purified by reversed-phase HPLC and characterized by ESI-MS, HRMS, and NMR spectra.

As a preliminary investigation, we synthesized **2** employing 1-(5-bromo-2-hydroxyphenyl)-1,3-butanedione as 1,3-dicarbonyl synthon in the Biginelli reaction. In particular, we first wondered whether substitutions on the aromatic ring at the C5 could gain favorable interactions with B:PHE44. Moreover, since in the proposed 3D model of **1**, the 6-ethylcarboxylate function was not involved in fundamental contacts in the binding site, this synthon could allow the replacement of this chemical function with the smaller 6-methyl group. Also, this chemical modification was encouraged by the presence of H-bond acceptors/donors (bromine and −OH in this case) on the precursor building block, with the aim to better accommodate this chemical function to reach the edge-to-face $\pi-\pi$ interaction with the protein residue counterpart (Figure S2, Supporting Information). In details, prior to synthesizing **2**, virtual docking experiments revealed the meta-position on the aromatic ring at C5 as the correct topology to mimic the chlorine of LVJ deeply inserted in the mPGES-1 binding cavity. The presence of a *meta*-bromine revealed a better predicted binding affinity if compared with the *meta*-chloro and *meta*-hydroxyl analogues. For all these reasons, among the commercially available building blocks, 1-(5-bromo-2-hydroxyphenyl)-1,3-butanedione was chosen as 1,3-dicarbonyl synthon, also for the further presence of a hydroxyl substituent able to establish polar interactions with the receptor counterpart. Docking studies of **2** showed a slightly better interaction of the (5-bromo-2-hydroxyphenyl)-oxo substituent at the C5 with B:PHE44, even if also in this case this group was not perfectly superimposed with that of LVJ involved in the $\pi-\pi$ with B:PHE44. In vitro biological tests confirmed these computational outcomes, with an IC_{50} = 5.60 ± 0.40 μM, comparable with that of **1** (IC_{50} = 4.16 ± 0.47 μM). We were intrigued by this data for the possibility of further optimizing the orientation of the aromatic moiety at C5, while conserving the methyl group at C6. Then, in order to achieve a more suitable orientation in the binding site, we decided to consider the simple phenyl ring at C5, but increasing its distance from the dihydropryrimidine core with the introduction of an oxymethylene spacer (Scheme 1), by using benzyl acetoacetate as 1,3-dicarbonyl synthon for the synthesis of compound **3**. Docking experiments supported this hypothesis, with a perfect superimposition of the dichlorophenyl part of LVJ and the benzyl-oxy-carbonyl portion at the C5 of **3**, which is able to establish the key edge-to-face $\pi-\pi$ with B:PHE44 (Figure S3, Supporting Information). Indeed, the inhibitory activity on mPGES-1 was improved, with an IC_{50} = 1.40 ± 0.60 μM for **3**. Once identified a better interacting chemical moiety at the C5

DOI: 10.1021/ml500433j
ACS Med. Chem. Lett. 2015, 6, 187−191

on the DHPM core, we also considered the possibility of modifying the N1 position oriented toward the external part of the protein. We noticed that in **3** this unsubstituted nitrogen was not involved in any key interactions with polar residues, and then we introduced a 2-carboxy-ethyl function at N1 (compound **4**, Figure 3), as suggested by molecular docking experiments performed on differently N1 substituted compounds. The improvement of the biological profile of **4** (IC_{50} = 0.41 ± 0.02 μM) completely agreed with computational predictions, confirming the hypothesis that the additional 2-carboxy-ethyl moiety at N1 gains relevant polar interactions, in particular with the key residue A:SER127. Notably, this key-residue contributes to the catalytic process behind the isomerization of PGH_2 to PGE_2[14] and is placed in a region of the protein (Chain A) in which LVJ (low-nanomolar activity range) is able to establish an additional H-bond network, thus explaining the difference in inhibitory activity with **4** (high nanomolar range). Moreover, the fulfillment of the key interactions with the receptor counterpart was found for both the possible enantiomers at C4, albeit a difference in predicted binding energies was observed due to the slightly different orientation of the dihydropyrimidine core into the mPGES-1 binding cavity (Figure S4, Supporting Information).

In conclusion, the careful analysis of mPGES-1 crystal structure in complex with the known inhibitor LVJ offered a direction for the more suitable decoration pattern on the previously reported dihydropyrimidine-based mPGES-1 inhibitors, disclosing **4** as a new potent compound. In fact, **4** inhibits mPGES-1 activity with IC_{50} = 0.41 ± 0.02 μM and is the most potent inhibitor that we have developed by rational design on the DHPM scaffold. The outlined structure−activity relationship here reported and the very useful synthetic approach represent an important point for the design of new promising focused collections of mPGES-1 inhibitors. In a future perspective, data and structural information here shown suggest an oriented virtual screening campaign of large libraries of synthetically accessible dihydropyrimidine-based compounds through the combinatorial Biginelli reaction.

■ ASSOCIATED CONTENT

Supporting Information

Computational details, molecular docking models, experimental procedures, characterization data, NMR-mass spectra. This material is available free of charge via the Internet at http://pubs.acs.org.

■ AUTHOR INFORMATION

Corresponding Authors

*Tel: +39 089 969741. Fax: +39 089 969602. E-mail: bifulco@unisa.it.

*Tel: +39 089 969743. E-mail: brunoin@unisa.it.

Author Contributions

All authors have given approval to the final version of the manuscript.

Funding

Financial support by Associazione Italiana Ricerca sul Cancro (AIRC) Grant IG_12777 (to G.B.).

Notes

The authors declare no competing financial interest.

■ ABBREVIATIONS

PGE_2, prostaglandin E_2; mPGES-1, microsomal PGE_2 synthase-1; mPGES-2, microsomal PGE_2 synthase-2; cPGES, cytosolic prostaglandin E_2 synthase-1; GSH, glutathione; COX, cyclooxygenase; NSAIDs, nonsteroidal anti-inflammatory drugs; IC_{50}, half maximal inhibitory concentration

■ REFERENCES

(1) Kudo, I.; Murakami, M. Prostaglandin E synthase, a terminal enzyme for prostaglandin E2 biosynthesis. *J. Biochem. Mol. Biol.* **2005**, *38*, 633−638.

(2) Samuelsson, B.; Morgenstern, R.; Jakobsson, P. J. Membrane prostaglandin E synthase-1: a novel therapeutic target. *Pharmacol. Rev.* **2007**, *59*, 207−224.

(3) Trebino, C. E.; Stock, J. L.; Gibbons, C. P.; Naiman, B. M.; Wachtmann, T. S.; Umland, J. P.; Pandher, K.; Lapointe, J. M.; Saha, S.; Roach, M. L.; Carter, D.; Thomas, N. A.; Durtschi, B. A.; McNeish, J. D.; Hambor, J. E.; Jakobsson, P. J.; Carty, T. J.; Perez, J. R.; Audoly, L. P. Impaired inflammatory and pain responses in mice lacking an inducible prostaglandin E synthase. *Proc. Natl. Acad. Sci. U.S.A.* **2003**, *100*, 9044−9049.

(4) Kamei, D.; Yamakawa, K.; Takegoshi, Y.; Mikami-Nakanishi, M.; Nakatani, Y.; Oh-Ishi, S.; Yasui, H.; Azuma, Y.; Hirasawa, N.; Ohuchi, K.; Kawaguchi, H.; Ishikawa, Y.; Ishii, T.; Uematsu, S.; Akira, S.; Murakami, M.; Kudo, I. Reduced pain hypersensitivity and inflammation in mice lacking microsomal prostaglandin E synthase-1. *J. Biol. Chem.* **2004**, *279*, 33684−33695.

(5) Engblom, D.; Saha, S.; Engström, L.; Westman, M.; Audoly, L. P.; Jakobsson, P. J.; Blomqvist, A. Microsomal prostaglandin E synthase-1 is the central switch during immune-induced pyresis. *Nat. Neurosci.* **2003**, *6*, 1137−1138.

(6) Westman, M.; Korotkova, M.; af Klint, E.; Stark, A.; Audoly, L. P.; Klareskog, L.; Ulfgren, A. K.; Jakobsson, P. J. Expression of microsomal prostaglandin E synthase 1 in rheumatoid arthritis synovium. *Arthritis Rheum.* **2004**, *50*, 1774−1780.

(7) Abdel-Magid, A. F. Prostaglandin E2 synthase-1 inhibitors as potential treatment for osteoarthritis. *ACS Med. Chem. Lett.* **2012**, *3*, 703−704.

(8) Kamei, D.; Murakami, M.; Nakatani, Y.; Ishikawa, Y.; Ishii, T.; Kudo, I. Potential role of microsomal prostaglandin E synthase-1 in tumorigenesis. *J. Biol. Chem.* **2003**, *278*, 19396−19405.

(9) Nakanishi, M.; Gokhale, V.; Meuillet, E. J.; Rosenberg, D. W. mPGES-1 as a target for cancer suppression: A comprehensive invited review "Phospholipase A2 and lipid mediators. *Biochimie* **2010**, *92*, 660−664.

(10) McGettigan, P.; Henry, D. Cardiovascular risk and inhibition of cyclooxygenase: a systematic review of the observational studies of selective and nonselective inhibitors of cyclooxygenase 2. *J. Am. Med. Assoc.* **2006**, *296*, 1633−1644.

(11) Cheng, Y.; Wang, M.; Yu, Y.; Lawson, J.; Funk, C. D.; Fitzgerald, G. A. Cyclooxygenases, microsomal prostaglandin E synthase-1, and cardiovascular function. *J. Clin. Invest.* **2006**, *116*, 1391−1399.

(12) Chang, H. H.; Meuillet, E. J. Identification and development of mPGES-1 inhibitors: where we are at? *Future Med. Chem.* **2011**, *3*, 1909−1934.

(13) De Simone, R.; Chini, M. G.; Bruno, I.; Riccio, R.; Mueller, D.; Werz, O.; Bifulco, G. Structure-based discovery of inhibitors of microsomal prostaglandin E2 synthase-1, 5-lipoxygenase and 5-lipoxygenase-activating protein: promising hits for the development of new anti-inflammatory agents. *J. Med. Chem.* **2011**, *54*, 1565−1575.

(14) Sjögren, T.; Nord, J.; Ek, M.; Johansson, P.; Liu, G.; Geschwindner, S. Crystal structure of microsomal prostaglandin E2 synthase provides insight into diversity in the MAPEG superfamily. *Proc. Natl. Acad. Sci. U.S.A.* **2013**, *110*, 3806−3811.

(15) Lauro, G.; Strocchia, M.; Terracciano, S.; Bruno, I.; Fischer, K.; Pergola, C.; Werz, O.; Riccio, R.; Bifulco, G. Exploration of the dihydropyrimidine scaffold for the development of new potential anti-

DOI: 10.1021/ml500433j
ACS Med. Chem. Lett. 2015, 6, 187−191

inflammatory agents blocking prostaglandin E2 synthase-1 enzyme (mPGES-1). *Eur. J. Med. Chem.* **2014**, *80*, 407−415.
(16) Li, D.; Howe, N.; Dukkipati, A.; Shah, S. T. A; Bax, B. D.; Edge, C.; Bridges, A.; Hardwicke, P.; Singh, O. M. P.; Giblin, G.; Pautsch, A.; Pfau, R.; Schnapp, G.; Wang, M.; Olieric, V.; Caffrey, M. Crystallizing membrane proteins in the lipidic mesophase. Experience with human prostaglandin E2 synthase 1 and an evolving strategy. *Cryst. Growth Des.* **2014**, *14*, 2034−2047.
(17) Dallinger, D.; Kappe, C. O. Creating chemical diversity space by scaffold decoration of dihydropyrimidines. *Pure Appl. Chem.* **2005**, *77*, 155−161.
(18) Kappe, C. O. Biologically active dihydropyrimidones of the Biginelli −type-a literature survey. *Eur. J. Med. Chem.* **2000**, *35*, 1043−1052.
(19) Pisani, L.; Prokopcovà, H.; Kremsner, J. M.; Kappe, C. O. 5-Aroyl-3,4-dihydropyrimidin-2-one library generation via automated sequential and parallel microwave-assisted synthesis techniques. *J. Comb. Chem.* **2007**, *9*, 415−421.

DOI: 10.1021/ml500433j
ACS Med. Chem. Lett. 2015, 6, 187−191